ANESTHESIOLOGY

Propofol Anesthesia Increases Long-range Frontoparietal Corticocortical Interaction in the Oculomotor Circuit in Macaque Monkeys

Li Ma, B.S., Wentai Liu, Ph.D., Andrew E. Hudson, M.D., Ph.D.

ANESTHESIOLOGY 2019; 130:560–71

EDITOR'S PERSPECTIVE

What We Already Know about This Topic

- A decrease in frontoparietal functional connectivity has been demonstrated with multiple anesthetic agents, and this decrease has been proposed as a final common functional pathway to produce anesthesia.
- Two alternative measures of long-range cortical interaction are coherence and phase-amplitude coupling. Although phase-amplitude coupling within frontal cortex changes with propofol administration, the effects of propofol on phase-amplitude coupling between different cortical areas have not previously been reported.

What This Article Tells Us That Is New

- Using a previously published monkey electrocorticography data set, it was found that propofol induced coherent slow oscillations in visual and oculomotor networks made up of cortical areas with strong anatomic projections.
- Frontal eye field within-area phase-amplitude coupling increased.
- Contrary to expectations from previous functional connectivity studies, interareal phase-amplitude coupling also increased with propofol.

ABSTRACT

Background: Frontoparietal functional connectivity decreases with multiple anesthetics using electrophysiology and functional imaging. This decrease has been proposed as a final common functional pathway to produce anesthesia. Two alternative measures of long-range cortical interaction are coherence and phase-amplitude coupling. Although phase-amplitude coupling within frontal cortex changes with propofol administration, the effects of propofol on phase-amplitude coupling between different cortical areas have not previously been reported. Based on phase-amplitude coupling observed within frontal lobe during the anesthetized period, it was hypothesized that between-lead phase-amplitude coupling analysis should decrease between frontal and parietal leads during propofol anesthesia.

Methods: A published monkey electrocorticography data set (N = 2 animals) was used to test for interactions in the cortical oculomotor circuit, which is robustly interconnected in primates, and in the visual system during propofol anesthesia using coherence and interarea phase-amplitude coupling.

Results: Propofol induces coherent slow oscillations in visual and oculomotor networks made up of cortical areas with strong anatomic projections. Frontal eye field within-area phase-amplitude coupling increases with a time course consistent with a bolus response to intravenous propofol (modulation index increase of 12.6-fold). Contrary to the hypothesis, interareal phase-amplitude coupling also increases with propofol, with the largest increase in phase-amplitude coupling in frontal eye field low-frequency phase modulating lateral intraparietal area β-power (27-fold increase) and visual area 2 low-frequency phase altering visual area 1 β-power (19-fold increase).

Conclusions: Propofol anesthesia induces coherent oscillations and increases certain frontoparietal interactions in oculomotor cortices. Frontal eye field and lateral intraparietal area show increased coherence and phase-amplitude coupling. Visual areas 2 and 1, which have similar anatomic projection patterns, show similar increases in phase-amplitude coupling, suggesting higher order feedback increases in influence during propofol anesthesia relative to wakefulness. This suggests that functional connectivity between frontal and parietal areas is not uniformly decreased by anesthetics.

(ANESTHESIOLOGY 2019; 130:560–71)

Multiple studies with multiple anesthetics report decreased corticocortical functional connectivity during general anesthesia, using both electrophysiology and functional magnetic resonance imaging.[1–5] A particularly attractive integration of these data is an hypothesis that anesthesia results from disruption of frontoparietal functional connectivity, which occurs even with agents that act on distinct receptor systems and hence might represent a final common functional pathway to produce an anesthetic state.[6,7]

Functional connectivity quantifies a probabilistic relationship between two signals: two signals are "functionally connected" if a signal at sensor A can be used to predict the signal from sensor B. This statistical relationship can result from a number of anatomic relationships. Cross-frequency coupling, including phase-amplitude coupling—or the gating of a high frequency oscillation's amplitude by the phase of a low frequency oscillation—has been proposed as a mechanism to modulate long-range neuronal communication and

This article is featured in "This Month in Anesthesiology," page 1A. Corresponding article on page 528.

Submitted for publication May 11, 2018. Accepted for publication January 10, 2019. From the School of Information Engineering, Wuhan University of Technology, Wuhan, China (L.M.); the Department of Bioengineering (L.M., W.L.), the California Nanosystems Institute (W.L.), the Department of Electrical and Computer Engineering (W.L.), and the Department of Anesthesiology and Perioperative Medicine (A.E.H.), University of California, Los Angeles, California.

hence functional connectivity.[8,9] Phase-amplitude coupling can be generically produced by interconnected populations of excitatory and inhibitory neurons[10] and can be observed between different frequency bands recorded in a single area or between two different areas. Within a single cortical area, propofol alters slow oscillation–α-band phase-amplitude coupling,[11] and propofol, sevoflurane, and ketamine have all been shown to increase δ–γ and θ–γ phase-amplitude coupling.[12] Interarea phase-amplitude coupling has not been widely reported in anesthesia studies to date, although it has been used in other contexts.[13]

Many studies of anesthetic effects on cortical functional connectivity have utilized electroencephalography data for practical reasons: electroencephalography is easy to record, is noninvasive, and shows characteristic shifts with anesthetic depth.[14] However, as a volume-averaged, low pass–filtered readout of the cortical areas underlying relatively large leads, electroencephalography has specific disadvantages for relating shifts in functional connectivity to anatomic connectivity.[15] More finely resolved electrocorticography data provided by smaller leads placed directly on the surface of cortex may offer a better scale for connectivity analyses. Although one can still critique electrocorticography as a macroscopic measure of neuronal activity, the main limitation of electrocorticography is its inherent invasiveness, which prevents the practical acquisition of such data from normal human brains.

Here we analyze data from a publically available repository of macaque monkey electrocorticography to ask whether propofol, which decreases frontoparietal functional connectivity, also dissociates activity in two cortical areas involved in oculomotor behavior that have particularly potent reciprocal anatomic projections: frontal eye field and lateral intraparietal area. This circuit seems appropriate to query with phase-amplitude coupling as stimulation of frontal eye field evokes γ-band oscillations within lateral intraparietal area.[16] To compare with other corticocortical interactions, we compare the relationships between frontal eye field and lateral intraparietal area to those with two occipital visual cortical areas, visual areas 1 and 2, which also project to frontal eye field and lateral intraparietal area. Counter the hypothesis of loss of frontoparietal connectivity, here we show that phase-amplitude coupling between frontal eye field and lateral intraparietal area increases during anesthesia produced by bolus intravenous administration of propofol, and a similar pattern occurs between visual areas 2 and 1.

Materials and Methods

Subjects and Data Recordings

This study analyzes previously published neurophysiology data from a publicly available repository, available *via* the Neurotycho website (http://neurotycho.org/; accessed February 20, 2018). For experimental details of data acquisition, the reader is referred to the original report, which includes the following statement: "All experimental and surgical procedures were performed in accordance with the experimental protocols (No. H24-2-203(4)) approved by the RIKEN ethics committee and the recommendations of the Weatherall report, 'The Use of Non-human Primates in Research.'"[17]

Briefly, high density electrocorticography signals were recorded from two adult *Macaca fuscata* macaque monkeys (monkeys C and G) by investigators at the Brain Science Institute, RIKEN, Japan, using a subdural 128-channel electrocorticography electrode array (Unique Medical, Japan),[18] covering the cortical surface of the left hemisphere (fig. 1A). A reference electrode consisting of a rectangular platinum plate was placed in the subdural space between the electrocorticography array and dura mater, and a ground electrode was placed in the epidural space. Electrocorticography data were sampled at 1 kHz using a Cerebus data acquisition system (Blackrock, USA). The sample size was based on the available data.

Experimental Procedure

The monkeys were restrained in a primate chair with careful monitoring of heart rate and respiration throughout the experiment. For baseline data, recordings began with the animal awake with eyes open. After 10 to 20 min of data acquisition, the eyes were covered, and recording continued for another 10 to 20 min (fig. 1B). For the anesthesia period, a bolus dose of propofol (5 or 5.2 mg/kg) was injected intravenously. Loss of responsiveness was determined by hand manipulation and by touching the nostril and philtrum with a cotton swab. Slow-wave oscillations in the electrocorticography served as an additional confirmation of loss of consciousness. Recording continued until the monkey regained responsiveness to manipulation of the hand or stimulation of the philtrum with a cotton swab. After 10 to 20 min of recording with the eyes covered, the eye covering was removed, and a final period of data was acquired. For our analysis we compared the baseline eyes-closed state to the period of unconsciousness and the recovery state with eyes closed. Each monkey was administered propofol on two separate days.

Data Analysis

Electrocorticography signals were rereferenced using a common average. A tenth order notch filter (49 to 51 Hz) reduced line noise contamination, and the resulting data were detrended before analysis. Artifacts were detected by eye after *Z*-score normalization and excluded from further analysis.

Spectral Analysis

We computed spectrograms for 500 s after induction with propofol using the multitaper method as implemented in the Chronux toolbox.[19] For the analysis, spectral estimates

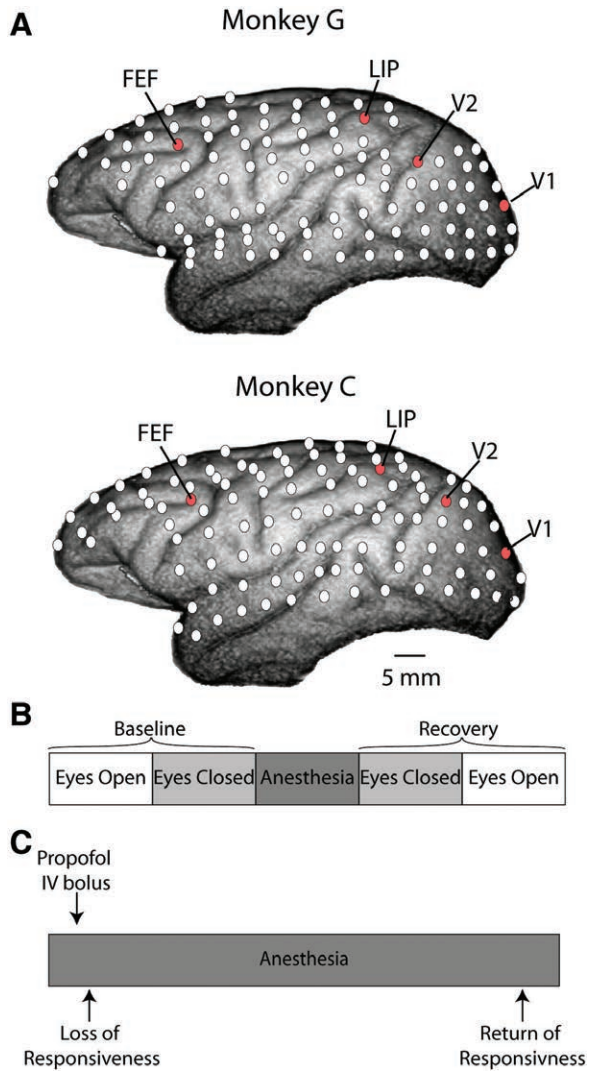

Fig. 1. Experimental design. (*A*) Representative electrocorticography leads were selected from each monkey's grid layout as indicated for further analysis. Note frontal eye field (FEF) and lateral intraparietal area (LIP) are separated by approximately 30 mm, and visual area 2 (V2) are separated by approximately 10 mm, and visual area 1 (V1) and V2 are separated by approximately 15 mm. (*B*) Block design. On each experimental day, baseline data were first recorded with eyes open, before covering the monkey's eyes with a blindfold. An anesthesia session was then recorded. After the monkey recovered responsiveness to somatosensory stimulation, the recovery period was then recorded in an eyes-closed epoch, and finally the blindfold was removed. (*C*) The anesthesia data was recorded to capturing the onset of a bolus dose of propofol (~5 mg kg^{-1}), with documentation of the time of loss of responsiveness to sensory stimulation and recovery of responsiveness to sensory stimulation. FEF, frontal eye field; IV, intravenous.

using 20-s sliding windows with a 1-s step were computed using seven tapers. Thus time resolution of our spectrograms is 20 s, and the frequency resolution is 0.4 Hz. After inspecting to confirm no artifacts contaminated the analysis, a group-level spectrogram was calculated by averaging over all experiments. Coherence offers one method for determining long-range cortical interactions.[20] Time-varying coherence, or cohereograms, were calculated similarly using the multitaper method with the same parameters and hence same time-frequency bandwidth.

Phase-amplitude Coupling

Phase-amplitude coupling (fig. 2) can be quantified by many methods,[13,21–27] each with specific advantages and disadvantages.[21,28] However, the Kullback–Leibler modulation index proposed by Tort *et al.*[28] performs better than or equivalent to other methods in terms of tolerance to noise, independence of amplitude, and sensitivity to modulation width and hence is used here. To quantify the modulation of the amplitude of activity in a high frequency band, f_A, as a function of the phase of the rhythm in a lower frequency band, f_p, modulation index is computed from a phase-amplitude histogram distribution, obtained as follows.

First, a raw signal $X_{raw}(t)$ is band pass filtered to obtain two frequency ranges for analysis: $x_{f_p}(t)$ and $x_{f_A}(t)$. The Hilbert transform is applied to the filtered signals $x_{f_p}(t)$ and $x_{f_A}(t)$ to extract the phase of $x_{f_p}(t)$ as $\varphi_{f_p}(t)$ and the amplitude of $x_{f_A}(t)$ as $A_{f_A}(t)$. Then the composite time series $\Psi\left[\varphi_{f_p}(t), A_{f_A}(t)\right]$ is constructed, which gives the amplitude of the oscillation f_A at each corresponding phase of the rhythm f_p. The phases φ_{f_p} are binned into j bins, and the mean of A_{f_A} over each phase bin j, $\left\langle \overline{A_{f_A}} \right\rangle_{\varphi f_{p,j}}$, is calculated and then normalized by dividing each bin value by the sum over the bins:

$$P(j) = \frac{\left\langle \overline{A_{f_A}} \right\rangle_{\varphi_{f_{p,j}}}}{\sum_{k}^{N} = 1 \left\langle \overline{A_{f_A}} \right\rangle \varphi_{f_{p,k}}}$$

where N is the number of phase bins. Note $P(J) \geq 0 \forall j$ and $\sum_{j=1}^{N} P(j) = 1$. This distribution-like function is referred to as the "amplitude distribution." It is obtained by plotting P as a function of the phase bin.

The modulation index is derived from the Kullback–Leibler divergence[29] between the observed $P(j)$ and the uniform distribution, because the amplitude distribution $P(j)$ over phase bins is expected to be uniform in the absence of phase-amplitude coupling. The Kullback–Leibler divergence of a discrete distribution P from a distribution Q is defined as follows:

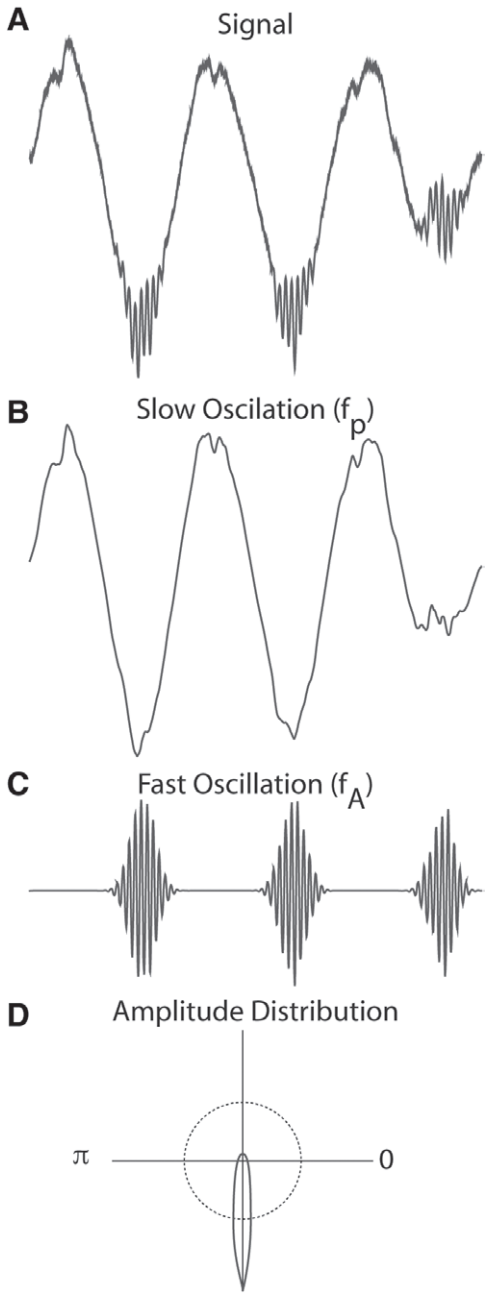

Fig. 2. Phase-amplitude coupling. (*A*) A signal with within-area phase-amplitude coupling. (*B*) A low-pass filtered version of signal A isolates the slow-wave envelope (f_p). (*C*) A bandpass filtered version of signal A isolates the faster oscillation (f_A). Phase-amplitude coupling is evident in that the amplitude of f_A is largest during one phase of f_p, the trough. (*D*) This can be clearly seen in the amplitude distribution, where the average amplitude of f_A is plotted as a function of the phase angle of f_p. These data demonstrate a large deviation from the uniform distribution (shown as the *dotted line*).

$$D_{KL}(P,Q)=\sum_{j=1}^{N}P(j)\log\left[\frac{P(j)}{Q(j)}\right]$$

Note that $D_{KL}(P,Q)\geq 0$ and $D_{KL}(P,Q)=0$ if and only if $P=Q$. Furthermore, D_{KL} is related to the Shannon entropy (H) of a distribution P:

$$H(P)=-\sum_{j=1}^{N}P(j)\log(P(j))$$

So, the Kullback–Leibler divergence between the observed $P(j)$ and the uniform distribution is:

$$D_{KL}(P,U)=\log(N)-H(P)$$

where U is the uniform distribution. Note that $\log(N)$ is the maximum entropy value possible over the discrete distribution, which only occurs for a uniform distribution.

The modulation index (MI) is calculated by dividing the Kullback–Leibler divergence of the observed P phase amplitude distribution from the uniform distribution by $\log(N)$:

$$MI=\frac{D_{KL}(P,U)}{\log(N)}$$

If the mean phase amplitude distribution is uniform over phase bin, $MI=0$ (*i.e.*, there is no coupling). If P is entirely concentrated in one bin like a Dirac δ distribution, then $MI=1$.

In this study, we filtered the electrocorticography signal to extract frequency bands of interests: slow-wave (0.1 to 1 Hz) and β-band (14–25 Hz) oscillations with *eegfilt* function implemented in EEGLab.[30] We computed modulation index by assigning each temporal sample to one of N = 18 equally spaced phase bins based on the instantaneous value of $\varphi_{f_p}(t)$ within a 2-min epoch. Note that the minimum data length needed for a reliable measurement depends on the frequency because slower oscillations will have fewer cycles sampled than faster rhythms.[28] To minimize the contamination of our phase-amplitude coupling calculation by response transients, we compared phase-amplitude coupling during the middle 2 min of each phase of the experiment.

Statistical Analysis

Modulation indices for all the frontal channels over three different stages are statistically compared for each experiment by two-tailed paired Student's t test with a significance criterion of $P < 0.05$. The stages include (1) preanesthesia baseline waking state, (2) anesthetic-induced unconsciousness, and (3) post-anesthetic recovery wakefulness. The 2-min time-resolved MI series (16 analysis

channels × 2 animals × 2 experiments) were bootstrapped to determine 95% CI (2,000 replicates) and averaged across all channels, subjects, and experiments for each time window. For cross-channel (frontal eye field, lateral intraparietal area, and visual areas 1 and 2) phase-amplitude coupling, we computed the four-channel coupling matrix for all subjects, constructed bootstrap 95% CI (2,000 replicates), and then averaged within experiment stage to obtain the mean cross-channel coupling matrix. All statistical analysis was performed in MatLab (Mathworks, USA). There were no missing data.

Results

To characterize the power spectral density response to bolus propofol administration, we computed average spectrograms aligned to the administration of propofol normalized to the pre-propofol baseline, eyes-closed spectrum.[31] These spectrograms revealed an early development of an ~1-Hz oscillation in frontal eye field with diffuse high frequency power approximately 30 s after the intravenous bolus that then decreases within 100 s (fig. 3A). At approximately 225 s postbolus, a slow oscillation returns with gradual return of higher frequency power. The lateral intraparietal area average spectrogram response aligned to the administration of propofol revealed a similar pattern (fig. 3B). Visual areas 1 and 2 averaged spectrograms revealed a similar low-frequency power pattern, with early termination of the intrinsic eyes-closed α-rhythm (fig. 3, C and D), although the magnitude of the shift in low-frequency power was substantially smaller than in the frontal and parietal channels.

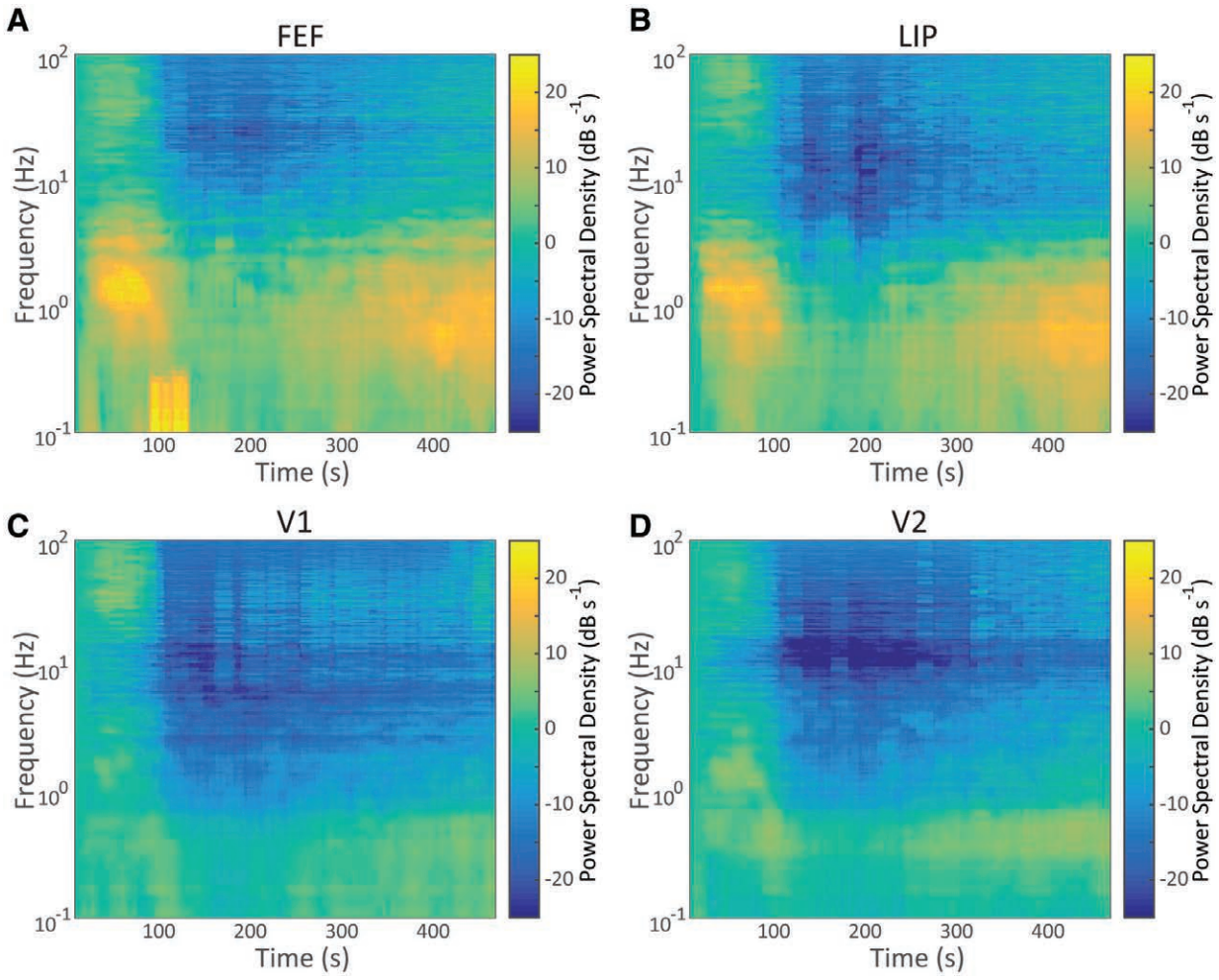

Fig. 3. Time evolution of effects of propofol on the power spectrum. Sliding window Thomson multitaper estimate of the spectrogram after intravenous (IV) bolus of propofol, by area: frontal eye field (FEF; *A*), lateral intraparietal area (LIP; *B*), visual area 1 (V1; *C*), and visual area 2 (V2; *D*). Each plot shows the averages across all animals and experimental sessions of the power spectral density as a function of frequency and time, aligned to the IV push of propofol. These estimates have a temporal resolution of 20 s and a 0.4-Hz frequency resolution.

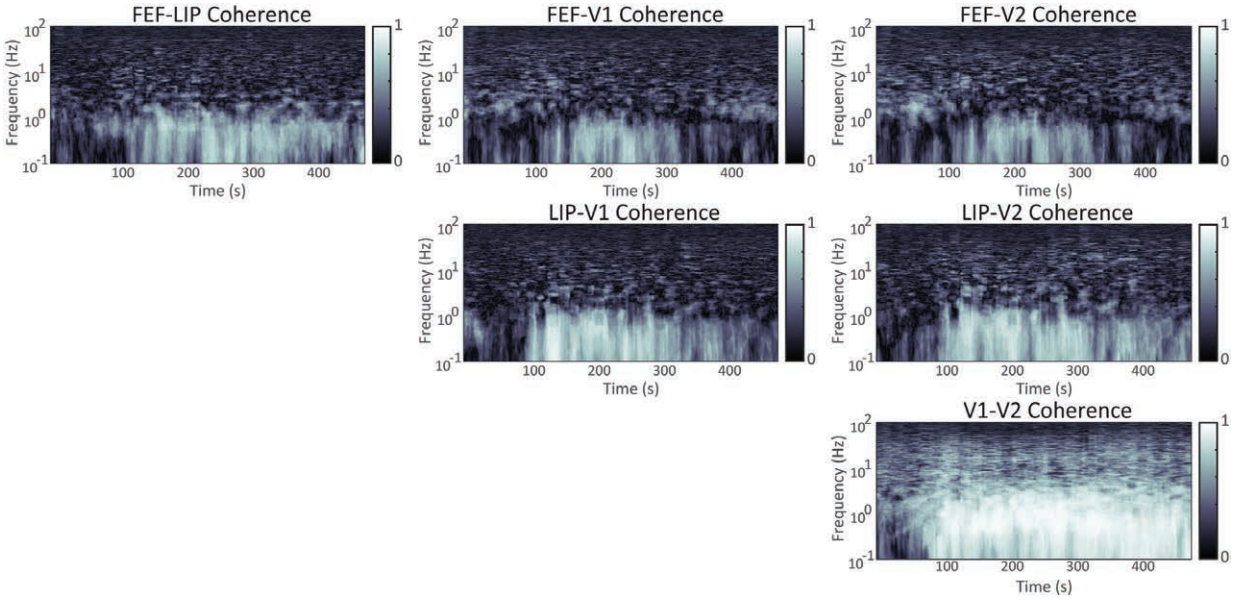

Fig. 4. Time evolution of coherence after propofol bolus. Mean over all subjects of sliding window multitaper estimate of coherence as a function of frequency and time after propofol bolus. Estimation parameters, and hence time and frequency resolution, are the same as figure 3: 20 s and 0.4 Hz. FEF, frontal eye field; LIP, lateral intraparietal area; V1, visual area 1; V2, visual area 2.

Coherent Slow Oscillations Occur in Anatomically Connected Regions of the Cortical Circuit during Propofol Anesthesia

The dominant feature in the average cohereograms after the propofol bolus is a peak in the slow-oscillation range. Coherence between frontal eye field and lateral intraparietal area and between visual areas 1 and 2 is established at 1 Hz before the low frequency power transient seen in the spectrogram decreases at 100 s (fig. 4). After approximately 100 s, the transient in the spectrogram has passed, and coherent slow-wave activity can be detected between all of the cortical areas tested (fig. 4) and persists for several hundred seconds. There is an additional coherence peak in the δ frequency range between frontal eye field–visual area 1 and frontal eye field–visual area 2 during the initial power transient response from roughly 50 to 75 seconds, but it does not recur until the slow oscillation coherence decreases approximately 400 s into the anesthetized period.

Bolus Intravenous Propofol Increases Within-lead Phase-amplitude Coupling

Propofol anesthesia has been reported to increase within-area phase-amplitude coupling.[12] We also find that propofol increases modulation index (fig. 5), and the modulation index returns to baseline with emergence from anesthesia within the frontal leads on the electrocorticography (fig. 5, A and C). This increase is most prominent between β-power (15 to 25 Hz) and the slow-oscillation (0.1 to 1 Hz) phase, as indicated by the boxes in figure 5 (A–C). Comparing the modulation index in this slow-oscillation β-range shows a significant elevation only during the propofol period (fig. 5D). The time course of the increased phase-amplitude coupling between β-power and the slow-oscillation phase is consistent with an impulse response to the IV bolus (fig. 5E).

IV Propofol Selectively Increases Between-lead Phase-amplitude Coupling, Consistent with Anatomic Connectivity

Given the presence of within-lead phase-amplitude coupling between the slow oscillation and β-activity, we chose this frequency pair to test for phase-amplitude coupling between the different oculomotor and visual cortical areas. We performed a 4 × 4 computation of cross-lead phase-amplitude coupling between frontal eye field, lateral intraparietal area, and visual areas 1 and 2 (fig. 6; table 1). During the anesthetized period (fig. 6B), the phase-amplitude coupling between the slow oscillation in frontal eye field and β-power in lateral intraparietal area was as high in magnitude as the within–lateral intraparietal area modulation of β-amplitude by slow-oscillation phase. The visual area 2 phase similarly showed a strong modulatory influence on visual area 1 β-power, with much lower average modulation index for other interactions. Again, by emergence the

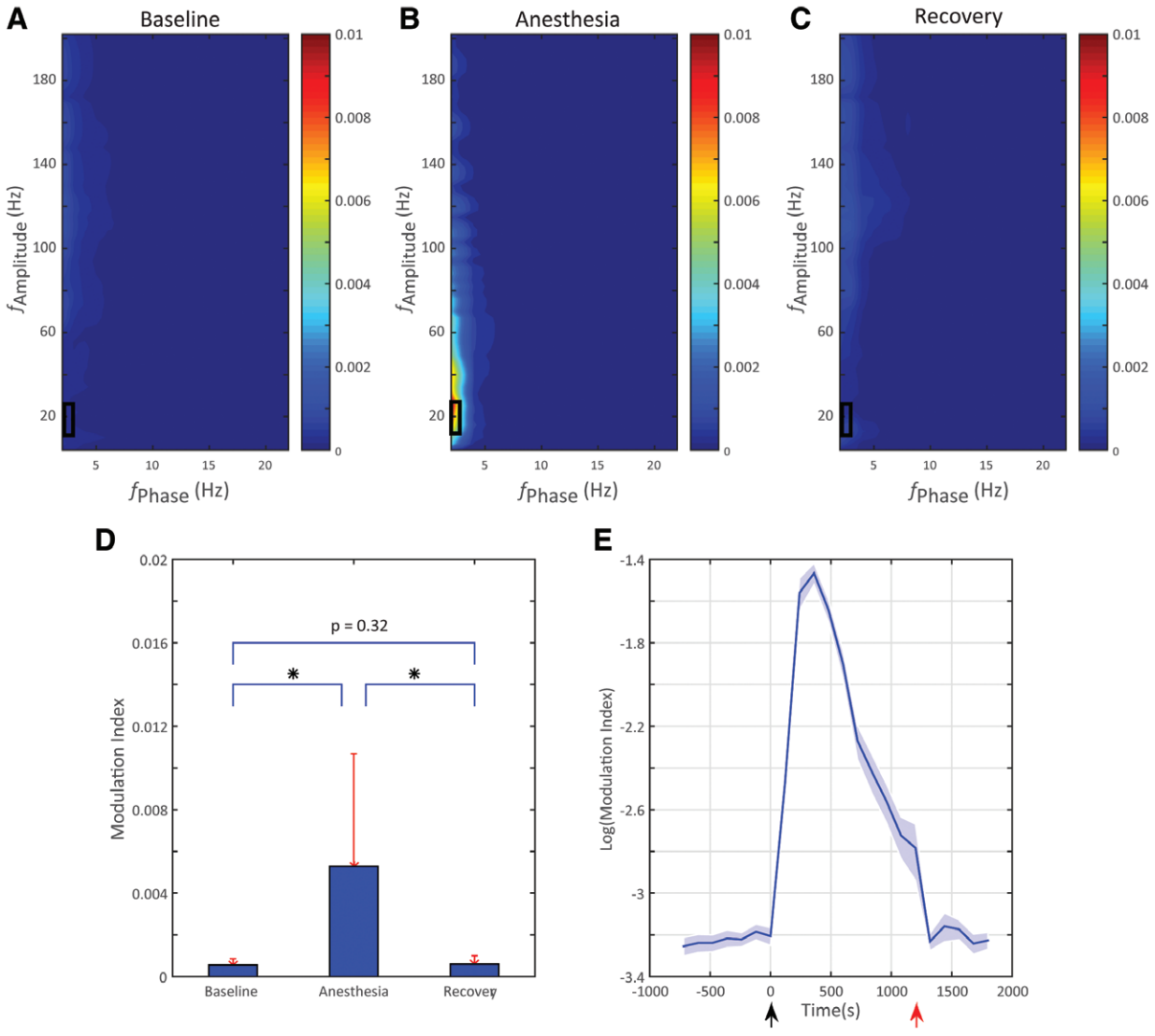

Fig. 5. Intraareal phase-amplitude coupling increases with propofol. (*A–C*) The mean comodulograms across frontal channels are shown for the baseline (*A*), the anesthetized period (*B*), and the recovery period (*C*). The slow oscillation phase modulating β-band amplitude during the anesthetized period is indicated by the *boxes*. (*D*) Slow-oscillation phase-β amplitude modulation index from the *boxed regions* of *A–C* over three stages across frontal channels. The values are shown as means, and *error bars* are SD. *Indicates $P < 0.05$. (*E*) Time course of frontal channel intraarea modulation index response to propofol calculated in 2-min increments. *Black arrow*, injection of anesthetic agent; *red arrow*, emergence from unconsciousness; *shaded area*, bootstrap 95% CI.

phase-amplitude coupling (fig. 6C) had essentially returned to baseline.

Discussion

Multiple electroencephalography studies have reported anesthetics, including propofol, functionally disconnect frontal cortical inputs from other cortical areas, particularly parietal lobe.[6,7] This drop in functional connectivity has been interpreted as suppression of cortical feedback contributing to the anesthetized state, which might suggest anesthetics selectively suppress synapses from higher-order areas. It has also been reported in human local field potential data that slow-wave oscillations are fragmented and incoherent at a distance.[32] However, here we show the opposite with electrocorticography: certain interactions, including coherent slow-wave oscillations and slow wave–β-phase–amplitude coupling, increase in cortical areas with known anatomic projections from one to the other.

Importantly, these increases in coupling between cortical areas appear to depend upon the projection anatomy. Coherence increases around 1 Hz occur earlier and persist

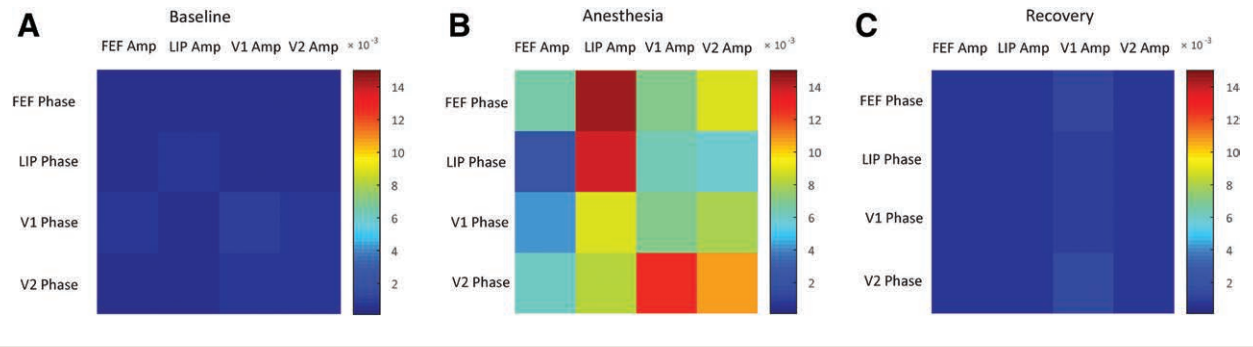

Fig. 6. Interareal phase amplitude (Amp) coupling increases with propofol. Mean of cross-channel modulation index between lateral intraparietal area (LIP), frontal eye field (FEF), visual area 1 (V1), and visual area 1 (V2) from all four experiments, by interval: baseline (*A*), anesthesia (*B*), and recovery (*C*). The strongest modulation is lateral intraparietal area β-amplitude modulated by frontal eye field slow-wave phase, followed by V1 β-amplitude modulated by V2 slow-wave phase. See table 1 for bootstrap confidence limits.

longer between frontal eye field and lateral intraparietal area and between visual areas 2 and 1 than between the visual and oculomotor cortices, and changes in interareal phase-amplitude coupling are largest with higher-order feedback projections, namely frontal eye field to lateral intraparietal area and visual areas 2 to 1. These coherent slow waves, recorded by electrodes separated by ~30 mm, contrast with the drop-in phase locking with distance previously reported with propofol anesthesia.[32] We have not computed phase locking factors between all possible leads for direct comparison to that study, but several observations may explain the differences. Lewis *et al.*[32] comment that low-frequency correlations that existed before the loss of consciousness persist or increase after loss of consciousness, so some coherence was observed in areas that were coherent before loss of consciousness, which was intermittently true between frontal eye field and lateral intraparietal area in our data. Lewis *et al.*[32] also did not compare electrodes to projection anatomy, which suggests that one way to reconcile this discrepancy might be to consider distance not in Euclidean terms but in terms of synaptic distance between two areas. On average, with a randomly placed electrode grid, the number of synapses between recorded neuronal populations will increase with the Euclidean distance between electrodes on the grid, but this relationship will occasionally be violated by long-range projections (that might not be robustly sampled by grids placed for clinical reasons). This would accord with several recent functional magnetic resonance imaging–based studies of functional connectivity during anesthesia that show that during anesthesia the functional connectivity maps show a diminished dynamic repertoire dominated by anatomical connectivity.[33,34]

Interareal phase-amplitude coupling should not be a surprise given the presence of within-area phase-amplitude coupling and coherence in the slow oscillation. Notably, however, these phase-amplitude coupling changes are markedly asymmetric, in that lateral intraparietal area slow-wave oscillation modulation of frontal eye field β-power and visual area 1 slow-wave oscillation modulation of visual area 2 β-power is not as prominent as the reverse (table 1). Thus phase-amplitude coupling between slow oscillation phase in the "higher order" cortical area and the β-amplitude in the "lower order" area increases during anesthesia, and that increase is larger than the phase-amplitude coupling seen in the reverse direction. This is the opposite of the predicted result from the frontoparietal connectivity hypothesis of general anesthesia.

Although all four of these cortical areas project to each other, there are differences in projection anatomy that mirror the observed asymmetry in the phase-amplitude coupling result. Frontal eye field has monosynaptic connections to lateral intraparietal area,[35] visual area 1,[36] and visual area 2.[37] The frontal eye field projection to lateral intraparietal area appears to involve all layers,[35] whereas the projection to visual area 2 targets layer 1 or 5/6.[37] The lateral intraparietal area has a reciprocal connection with frontal eye field.[38,39] Visual area 1 projects primarily to layer 4 of visual area 2, whereas projections from visual area 2 form primarily excitatory synapses in layers 1, 2/3, and 5.[40] Peripheral but not foveal visual area 2 projects to the lateral intraparietal area,[41] although other extrastriate visual areas are also closely connected with lateral intraparietal area.[42,43] Although it is tempting to attribute asymmetry in the phase-amplitude coupling results to differences in laminar projection pattern, more work needs to be done to identify the nature of the differences of the projection anatomy and then perturb those specific connections to test whether causality can be attributed to anatomy.

There are several interpretations of this discordance between our analysis and the functional connectivity data. Functional connectivity is a statistical relationship and hence separate from anatomic connectivity, namely, axons from cortical area A synapsing on neurons in cortical area B. The simplest case of functional connectivity decreases with anesthesia would be when the anesthetic decreases synaptic

Table 1. Interareal Phase-amplitude Coupling Variations

	Baseline				Anesthetized				Recovery			
Phase	FEF Amp	LIP Amp	V1 Amp	V2 Amp	FEF Amp	LIP Amp	V1 Amp	V2 Amp	FEF Amp	LIP Amp	V1 Amp	V2 Amp
FEF	5.4 (4.7–6.3)	5.4 (4.8–5.9)	5.4 (4.8–6.1)	5.5 (4.7–6.5)	68.1 (45.4–104.6)	145.9 (121.3–186.1)	68.0 (49.0–91.0)	89.7 (58.9–113.4)	6.5 (5.8–7.5)	6.9 (5.8–8.1)	13.5 (9.4–16.8)	6.7 (5.3–7.8)
LIP	5.5 (4.7–6.4)	5.9 (5.1–6.6)	5.6 (4.7–6.6)	5.7 (4.6–6.6)	23.2 (17.3–31.1)	138.8 (108.8–161.6)	61.0 (31.5–96.7)	57.8 (46.8–69.5)	6.5 (5.7–7.7)	6.6 (5.3–8.1)	10.6 (7.4–14.4)	5.8 (4.8–6.4)
V1	5.8 (5.0–6.7)	5.5 (4.6–6.5)	9.0 (7.4–10.8)	6.0 (5.3–6.9)	42.2 (28.8–57.0)	89.1 (56.7–122.9)	69.2 (46.0–89.1)	80.0 (61.1–103.7)	6.9 (5.4–8.4)	6.5 (5.5–7.5)	10.7 (8.0–12.5)	6.4 (5.5–7.4)
V2	4.8 (4.3–5.6)	5.4 (4.4–6.2)	6.6 (5.5–7.7)	5.7 (4.9–6.5)	62.0 (30.4–107.4)	82.0 (46.9–125.1)	126.0 (94.3–151.3)	109.2 (73.6–146.6)	6.7 (5.8–7.5)	6.1 (5.0–7.0)	15.7 (10.5–20.7)	7.0 (6.0–8.3)

The values are means (95% CI). CI values are computed using the bootstrap method (2,000 replicates). All values are modulation indices $\times 10^{-4}$. Coupling strength increases dramatically under anesthesia.
Amp, amplitude; FEF, frontal eye field; LIP, lateral intraparietal area; V1, visual area 1; V2, visual area 2.

transmission between two anatomically connected areas. In this case, however, we would expect phase-amplitude coupling between A and B to decrease during anesthesia, contrary to what we observe. Alternatively, functional connectivity does not need to arise from anatomic connectivity between A and B. Two examples of this are shown in figure 7: if a third area C projects to and influences firing in areas A and B, then A and B will be functionally connected even though the coupling does not occur through a direct anatomic projection; or if the connection between A and B results from a cascade, where area A affects area C, which then affects area B. Thus, the drop in frontoparietal functional connectivity detected with anesthesia might result from suppression of an input common to both areas, such as a brainstem or thalamic modulatory input, or it might result from degradation of communication along a relay cascade. Dropout of frontoparietal functional connectivity measured with electroencephalography between dorsolateral prefrontal cortex and inferior parietal lobule was shown together with functional magnetic resonance imaging evidence for suppression of an intermediate area, dorsal anterior insula by Warnaby *et al.*[5] This suggests that suppression of intervening projections (including insula, thalamus, and brainstem) might contribute to the reported decrease in frontoparietal functional connectivity with anesthesia when cortical areas do not have dense direct projections between them. Finally, although perhaps less likely, the filtered and volume averaged electroencephalography may simply show more functional connectivity at baseline than the more focal electrocorticography, and the

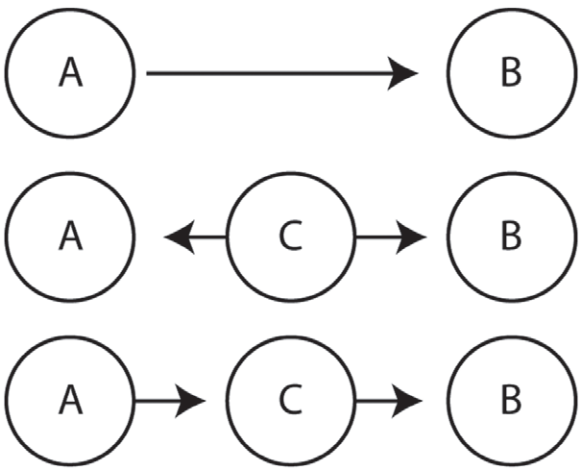

Fig. 7. Network coupling architecture. Networks that can produce coupling between two neuron populations, A and B. Although anatomic projections between A and B will produce detectable functional connectivity, functional connectivity could also be detected if a common area C projects to both A and B or if a cascade of connections exists such that A projects to C which then projects to B.

resultant averaging could blur out most of the increased interaction that we report in this article.

It is unlikely that the observed effect is a signal processing artifact. Although within area δ–γ and θ–γ phase-amplitude coupling has been reported to increase with anesthesia,[12] the interareal slow wave–β-phase–amplitude coupling increase we observe is of the same magnitude or larger than the within-area slow wave–β-phase–amplitude coupling increase we see in these areas. The increase in phase-amplitude coupling follows a time course that matches the expected bolus response to IV administration of an anesthetic and returns to baseline by the time the animal has emerged from anesthesia. Increases in phase-amplitude coupling are directional and consistently larger from a "higher order" area to a "lower order" area, and they are not universal—the visual occipital areas show minimal phase-amplitude coupling with the oculomotor frontal and parietal areas, despite comparable physical distances between the locations.

A potential limitation of this report stems from our reliance on an existing published electrocorticography data set, with only four propofol experiments, although two administrations were performed in two animals. As a result, we cannot fully characterize the full population variability in the responsiveness of phase-amplitude coupling as a measure of corticocortical interaction during anesthesia, but there was no instance in which the rise in phase-amplitude coupling between frontal eye field and lateral intraparietal area or between visual areas 2 and 1 was absent. Additionally, because our analysis was limited to propofol, which has previously been shown to affect phase-amplitude coupling, the observed increase in phase-amplitude coupling between frontal eye field and lateral intraparietal area and visual areas 2 to 1 may represent drug-specific effects rather than correlates of the anesthetized state *per se*.

Limitations in our approach notwithstanding, our observations complicate current theories of anesthesia that posit a suppression of frontoparietal interactions produces the anesthetized state. Although this theory may prove true for nonspecific interactions between frontal and parietal regions, anatomically connected areas show increased interactions as measured by phase-amplitude coupling during propofol anesthesia. This effect is directional, in a fashion that correlates with the laminar nature of known anatomic projections, suggesting that γ-aminobutyric acid–mediated agents like propofol may differentially disturb processing in different cortical lamina.

Significantly, frontal eye field is part of dorsolateral prefrontal cortex, which is hypothesized to be central to the conscious perception of stimuli.[44] Certainly the frontal eye field and lateral intraparietal area are involved in visual working memory and attention,[45–47] which are necessary for the transition from phenomenal to access consciousness.[48,49] The ability of propofol to alter coupling between frontal eye field and lateral intraparietal area thus might be key to the disruption of conscious experience. We have shown that propofol induces an interaction between frontal eye field and lateral intraparietal area that is absent during conscious states. One could hypothesize that this aberrant coupling prevents frontal eye field from stabilizing distributed representations across multiple cortical areas and hence precludes the dynamic formation of multiple cortical areas into transient assemblies conjectured to underlie conscious perception. Further work is necessary to understand how increased phase-amplitude coupling relates to drops in functional connectivity previously reported with multiple anesthetics and multiple methodologies.

Research Support

Supported by National Natural Science Foundation of China (Beijing, China) grant No. 51675389 (to Dr. Ma), grants from California Capital Equity LLC (Culver City, California; to Dr. Liu) and National Institute of General Medical Sciences (Bethesda, Maryland) grant No. 1K08GM121961 (to Dr. Hudson).

Competing Interests

The authors declare no competing interests.

Correspondence

Address correspondence to Dr. Hudson: 757 Westwood Plaza, Suite 3325, Los Angeles, California 90095. ahudson@mednet.ucla.edu. This article may be accessed for personal use at no charge through the Journal Web site, www.anesthesiology.org.

References

1. Jordan D, Ilg R, Riedl V, Schorer A, Grimberg S, Neufang S, Omerovic A, Berger S, Untergehrer G, Preibisch C, Schulz E, Schuster T, Schröter M, Spoormaker V, Zimmer C, Hemmer B, Wohlschläger A, Kochs EF, Schneider G: Simultaneous electroencephalographic and functional magnetic resonance imaging indicate impaired cortical top-down processing in association with anesthetic-induced unconsciousness. Anesthesiology 2013; 119:1031–42
2. Palanca BJ, Mitra A, Larson-Prior L, Snyder AZ, Avidan MS, Raichle ME: Resting-state functional magnetic resonance imaging correlates of sevoflurane-induced unconsciousness. Anesthesiology 2015; 123:346–56
3. Boveroux P, Vanhaudenhuyse A, Bruno MA, Noirhomme Q, Lauwick S, Luxen A, Degueldre C, Plenevaux A, Schnakers C, Phillips C, Brichant JF, Bonhomme V, Maquet P, Greicius MD, Laureys S, Boly M: Breakdown of within- and between-network resting state functional magnetic resonance imaging connectivity during propofol-induced loss of consciousness. Anesthesiology 2010; 113:1038–53

4. Ranft A, Golkowski D, Kiel T, Riedl V, Kohl P, Rohrer G, Pientka J, Berger S, Thul A, Maurer M, Preibisch C, Zimmer C, Mashour GA, Kochs EF, Jordan D, Ilg R: Neural correlates of sevoflurane-induced unconsciousness identified by simultaneous functional magnetic resonance imaging and electroencephalography. Anesthesiology 2016; 125:861–72
5. Warnaby CE, Seretny M, Ní Mhuircheartaigh R, Rogers R, Jbabdi S, Sleigh J, Tracey I: Anesthesia-induced suppression of human dorsal anterior insula responsivity at loss of volitional behavioral response. Anesthesiology 2016; 124:766–78
6. Ku SW, Lee U, Noh GJ, Jun IG, Mashour GA: Preferential inhibition of frontal-to-parietal feedback connectivity is a neurophysiologic correlate of general anesthesia in surgical patients. PLoS One 2011; 6:e25155
7. Lee U, Ku S, Noh G, Baek S, Choi B, Mashour GA: Disruption of frontal-parietal communication by ketamine, propofol, and sevoflurane. Anesthesiology 2013; 118:1264–75
8. Meij R van der, Kahana M, Maris E: Phase-amplitude coupling in human electrocorticography is spatially distributed and phase diverse. J Neurosci 2012; 32:111–23
9. Canolty RT, Knight RT: The functional role of cross-frequency coupling. Trends Cogn Sci 2010; 14:506–15
10. Onslow AC, Jones MW, Bogacz R: A canonical circuit for generating phase-amplitude coupling. PLoS One 2014; 9:e102591
11. Mukamel EA, Pirondini E, Babadi B, Wong KF, Pierce ET, Harrell PG, Walsh JL, Salazar-Gomez AF, Cash SS, Eskandar EN, Weiner VS, Brown EN, Purdon PL: A transition in brain state during propofol-induced unconsciousness. J Neurosci 2014; 34:839–45
12. Pal D, Silverstein BH, Sharba L, Li D, Hambrecht-Wiedbusch VS, Hudetz AG, Mashour GA: Propofol, sevoflurane, and ketamine Induce a reversible increase in δ–γ and θ–γ phase-amplitude coupling in frontal cortex of rat. Front Syst Neurosci 2017; 11:41
13. Bruns A, Eckhorn R: Task-related coupling from high- to low-frequency signals among visual cortical areas in human subdural recordings. Int J Psychophysiol 2004; 51:97–116
14. Brown EN, Lydic R, Schiff ND: General anesthesia, sleep, and coma. N Engl J Med 2010; 363:2638–50
15. Nunez PL, Srinivasan R: Electric Fields of the Brain: The Neurophysics of EEG. New York, Oxford University Press, 2006
16. Premereur E, Vanduffel W, Roelfsema PR, Janssen P: Frontal eye field microstimulation induces task-dependent γ oscillations in the lateral intraparietal area. J Neurophysiol 2012; 108:1392–402
17. Yanagawa T, Chao ZC, Hasegawa N, Fujii N: Large-scale information flow in conscious and unconscious states: An ECoG study in monkeys. PLoS One 2013; 8:e80845
18. Nagasaka Y, Shimoda K, Fujii N: Multidimensional recording (MDR) and data sharing: An ecological open research and educational platform for neuroscience. PLoS One 2011; 6:e22561
19. Bokil H, Andrews P, Kulkarni JE, Mehta S, Mitra PP: Chronux: A platform for analyzing neural signals. J Neurosci Methods 2010; 192:146–51
20. Malekmohammadi M, AuYong N, Price CM, Tsolaki E, Hudson AE, Pouratian N: Propofol-induced changes in α-β sensorimotor cortical connectivity. Anesthesiology 2018; 128:305–16
21. Cohen MX: Assessing transient cross-frequency coupling in EEG data. J Neurosci Methods 2008; 168:494–9
22. Kramer MA, Eden UT: Assessment of cross-frequency coupling with confidence using generalized linear models. J Neurosci Methods 2013; 220:64–74
23. Miyakoshi M, Delorme A, Mullen T, Kojima K, Makeig S, Asano E: Automated detection of cross-frequency coupling in the electrocorticogram for clinical inspection. Conf Proc IEEE Eng Med Biol Soc 2013; 2013:3282–5
24. Colgin LL, Denninger T, Fyhn M, Hafting T, Bonnevie T, Jensen O, Moser MB, Moser EI: Frequency of γ oscillations routes flow of information in the hippocampus. Nature 2009; 462:353–7
25. Canolty RT, Edwards E, Dalal SS, Soltani M, Nagarajan SS, Kirsch HE, Berger MS, Barbaro NM, Knight RT: High γ power is phase-locked to θ oscillations in human neocortex. Science 2006; 313:1626–8
26. Amiri M, Frauscher B, Gotman J: Phase-amplitude coupling is elevated in deep sleep and in the onset zone of focal epileptic seizures. Front Hum Neurosci 2016; 10:387
27. Penny WD, Duzel E, Miller KJ, Ojemann JG: Testing for nested oscillation. J Neurosci Methods 2008; 174:50–61
28. Tort AB, Komorowski R, Eichenbaum H, Kopell N: Measuring phase-amplitude coupling between neuronal oscillations of different frequencies. J Neurophysiol 2010; 104:1195–210
29. Kullback S, Leibler RA: On information and sufficiency. Ann Math Stat 1951; 22:79–86
30. Delorme A, Makeig S: EEGLAB: An open source toolbox for analysis of single-trial EEG dynamics including independent component analysis. J Neurosci Methods 2004; 134:9–21
31. Hudson AE: Metastability of neuronal dynamics during general anesthesia: Time for a change in our assumptions? Front Neural Circuits 2017; 11:58
32. Lewis LD, Weiner VS, Mukamel EA, Donoghue JA, Eskandar EN, Madsen JR, Anderson WS, Hochberg LR, Cash SS, Brown EN, Purdon PL: Rapid fragmentation of neuronal networks at the onset of propofol-induced unconsciousness. Proc Natl Acad Sci U S A 2012; 109:E3377–86

33. Barttfeld P, Bekinschtein TA, Salles A, Stamatakis EA, Adapa R, Menon DK, Sigman M: Factoring the brain signatures of anesthesia concentration and level of arousal across individuals. Neuroimage Clin 2015; 9:385–91
34. Uhrig L, Sitt JD, Jacob A, Tasserie J, Barttfeld P, Dupont M, Dehaene S, Jarraya B: Resting-state dynamics as a cortical signature of anesthesia in monkeys. Anesthesiology 2018; 129:942–58
35. Anderson JC, Kennedy H, Martin KA: Pathways of attention: Synaptic relationships of frontal eye field to V4, lateral intraparietal cortex, and area 46 in macaque monkey. J Neurosci 2011; 31:10872–81
36. Clavagnier S, Falchier A, Kennedy H: Long-distance feedback projections to area V1: Implications for multisensory integration, spatial awareness, and visual consciousness. Cogn Affect Behav Neurosci 2004; 4:117–26
37. Stanton GB, Bruce CJ, Goldberg ME: Topography of projections to posterior cortical areas from the macaque frontal eye fields. J Comp Neurol 1995; 353:291–305
38. Ferraina S, Paré M, Wurtz RH: Comparison of cortico-cortical and cortico-collicular signals for the generation of saccadic eye movements. J Neurophysiol 2002; 87:845–58
39. Schall JD: Visuomotor areas of the frontal lobe, Cerebral Cortex. 1997, pp 527–638
40. Anderson JC, Martin KA: The synaptic connections between cortical areas V1 and V2 in macaque monkey. J Neurosci 2009; 29:11283–93
41. Baizer JS, Ungerleider LG, Desimone R: Organization of visual inputs to the inferior temporal and posterior parietal cortex in macaques. J Neurosci 1991; 11: 168–90
42. Andersen RA, Asanuma C, Essick G, Siegel RM: Corticocortical connections of anatomically and physiologically defined subdivisions within the inferior parietal lobule. J Comp Neurol 1990; 296:65–113
43. Blatt GJ, Andersen RA, Stoner GR: Visual receptive field organization and cortico-cortical connections of the lateral intraparietal area (area LIP) in the macaque. J Comp Neurol 1990; 299:421–45
44. Vugt B van, Dagnino B, Vartak D, Safaai H, Panzeri S, Dehaene S, Roelfsema PR: The threshold for conscious report: Signal loss and response bias in visual and frontal cortex. Science 2018; 360:537–42
45. Noudoost B, Chang MH, Steinmetz NA, Moore T: Top-down control of visual attention. Curr Opin Neurobiol 2010; 20:183–90
46. Clark KL, Noudoost B, Moore T: Persistent spatial information in the frontal eye field during object-based short-term memory. J Neurosci 2012; 32: 10907–14
47. Heinen K, Feredoes E, Ruff CC, Driver J: Functional connectivity between prefrontal and parietal cortex drives visuo-spatial attention shifts. Neuropsychologia 2017; 99:81–91
48. Chica AB, Bartolomeo P: Attentional routes to conscious perception. Front Psychol 2012; 3:1
49. Chica AB, Valero-Cabré A, Paz-Alonso PM, Bartolomeo P: Causal contributions of the left frontal eye field to conscious perception. Cereb Cortex 2014; 24: 745–53